Is fine sediment in sandy riverbed deposits a proxy for paleo-sediment supply?

Nathaniel Wysocki[1] and Elizabeth Hajek[1,*]

[1]Department of Geosciences, Pennsylvania State University, 503 Deike Building, University Park, PA 16802

**Corresponding Author*

ABSTRACT

The amount of silt and clay supplied to rivers can be a primary control on the form and dynamics of channel networks, and it affects the distribution and interconnectedness of buried fluvial reservoirs. Despite its importance, it is difficult to reconstruct how much fine sediment was supplied to ancient rivers. The presence of silt and clay accumulations in sandy river deposits is often interpreted as an indication of variability in flow conditions due to seasonal stagnation or tidal influence, but it has not been tested whether these deposits can be used to evaluate how much fine sediment was transported in ancient rivers. Here we report results from a series of experiments designed to evaluate how much clay and silt are preserved in sandy riverbed deposits under constant and variable discharge conditions. Our results demonstrate that 1) clay-silt deposits, including drapes and lenses, form under constant high-discharge conditions, 2) the amount of fine sediment recovered from bed-material deposits is higher when more fine sediment is supplied, and 3) the fraction of fine sediment trapped during bed aggradation is higher than what is retained during bypass conditions. These results confirm that fine-sediment accumulations are not unique indicators of variable flow conditions and that the net retention of

clay and silt in sandy riverbed deposits may be more indicative of the overall amount of fine sediment supplied to a river.

INTRODUCTION

Understanding how clay and silt are deposited and stored in riverbed sediments is important for a range of geologic and river-management issues. In modern rivers, the amount and distribution of fine sediment in riverbeds impacts riverine habitats, contaminant transport and leaching, and engineering decisions (e.g., Downs et al., 2009; Draut and Ritchie, 2015; Hamm et al., 2011; Packman and Brooks, 2001; Wooster et al., 2008). In ancient deposits, the abundance and distribution of mud accumulations control the quality and connectivity of fluvial aquifers and hydrocarbon reservoirs (e.g., Bierkens and Weerts, 1994; Jackson et al., 2005), and are useful for interpreting paleoenvironmental conditions in ancient fluvial systems, including the variability or seasonality of discharge (e.g., Plink-Bjorklund, 2015) and the long-term balance of sediment accumulation relative to river mobility (e.g., Hampson et al., 2012). Additionally, there are important outstanding questions about the influence of clays on channel dynamics (e.g., Matsubara et al., 2015). The ability to reconstruct the relative abundance of clay supplied to ancient rivers on Earth or other planets would help answer these questions and improve paleoenvironmental reconstructions from sedimentary deposits.

Because fine sediment can be transported with relatively low flow velocities and has a slow settling velocity, clay and fine silt accumulations in channel-bed deposits are often interpreted as indicating periods of very low flow or standing water. Consequently, clay drapes and lenses within ancient channel deposits are commonly cited as evidence of tidal influence, seasonal stagnation, or waning flows (e.g., Bhattacharya, 1997; Martin, 2000; Plink-Bjorklund, 2015; Steel et al., 2011). However, studies have shown that fine sediment can be incorporated into porous beds under high discharge conditions (e.g., Baas et al., 2016; Packman and MacKay, 2003). This raises the question of how to differentiate fine-sediment accumulations formed under variable or low discharge from those deposited under higher discharge conditions. Furthermore, if fine sediments are routinely incorporated into fluvial bed material under a range of flow conditions, the fraction of fine sediment preserved in ancient fluvial deposits may be useful for reconstructing the proportion of fines supplied to ancient river systems.

The presence of fine sediment can significantly influence sediment transport and flow conditions in channels. High clay concentrations can alter the structure of turbulent flows, suppressing turbulence completely when concentrations are high enough, and clay in channel beds can increase the effective shear stress necessary to erode the bed (Baas et al., 2016). Together these effects can change the scale, shape, and migration rate of bedforms, and ultimately may influence the character of sedimentary deposits from flows with high clay loads (e.g., Baas et al., 2011). The stratigraphic manifestation of the effects of clay on bedform morphodynamics is still being evaluated. In particular, for fully turbulent flows, it remains unclear whether differences in supplied clay concentrations in can be recorded in bed-material deposits formed under constant discharge.

We conducted a series of experiments to evaluate whether clay deposition occurs in sandy river beds under fully turbulent high-discharge conditions, and whether the amount of clay found in bed deposits is related to the amount of clay supplied to the flow. The experiments were designed to explore whether the amount of fine-sediment supplied to a flow affects the amount and distribution of fine-sediment accumulations in the bed and whether variable flow conditions significantly enhance the amount of fine-sediment deposited and stored in sandy river beds.

EXPERIMENTAL DESIGN

We performed a series of five experiments in a feed-style flume at the St. Anthony Falls Laboratory (University of Minnesota; Figure 1). Water and sediment discharge were set to aggrade a sand bed via a wedge of sediment that prograded down the flume during each run; this is analogous to a bar with superposed bedforms migrating downstream in a river. Sand (D_{50}=0.343 mm) and kaolin clay (D_{50}= 0.004 mm) were supplied to the flume at a constant rate. A clay slurry, with different concentrations for each run, was added to the flume at a rate of 1 l/s. Total water discharge for each run was 21 l/s and was monitored an acoustic Doppler velocimeter (ADV) and by measuring the water depth over the weir at the end of the flume. Water exited the end of the flume over a weir that was fixed, allowing the bed to aggrade during each run. Sand discharge was set at 15.0 g/s in all runs. The bed aggraded to the weir elevation in about four hours and each run was continued at bypass for 15 to 30 minutes.

Three runs had constant water discharge but different clay concentrations and one run had variable water discharge (Table). Discharge for all runs was sufficient to transport clay as wash load and the sand was transported in the suspended-load regime, consistent with natural sand bed systems where bed material $D_{50} \leq 0.50$ mm is often transported in suspension (Wilkerson and Parker, 2011) and all runs were equivalent to the fully turbulent flows of Baas et al. (e.g., 2016). The four constant-discharge runs had clay concentrations of 0.0, 1000, 4000, 8500 mg/l. The variable-discharge experiment had low clay concentration (1000 mg/l) and water and sediment discharge were slowed and stopped every hour, allowing fine sediment to settle onto the bed.

Each run was recorded from the side of the flume with a video camera and photographs. These images were used to reconstruct bed topography and measure bed aggradation and bedform scale in each run. After each experiment, the bed was dried for two days then excavated. Fine-sediment accumulations were mapped on photographs of the flume wall and samples were collected from bed deposits that accumulated during the aggradational and bypass phases of the experiment. Sediment samples were wet-sieved to determine the fraction of fine sediment. These values were combined with mapped fines accumulations to compare the amount of clay deposited in the bed throughout each run.

Experimental parameters and analyses are detailed in Supplementary Material along with links to videos of each run.

RESULTS

Fine-sediment accumulations in experimental bed deposits included lenses, drapes, and intercalated (interstitial) fines (Figure 2). Visible clay accumulations were most prominent in deposits from the high-concentration run, with most of the bed showing intercalated fines and numerous bedform-scale lenses and continuous drapes of fine sediment. Interstitial clay was less noticeable in the intermediate-discharge run, but bed deposits contained clay lenses and some continuous clay drapes. Bed deposits from the low-concentration run contained some clay drapes. Discontinuous clay drapes formed in deposits of the variable discharge run.

The proportion of clay in bed-material deposits increased with higher clay concentrations (Table). For all but the low-concentration constant-discharge run, the weight percent of clay significantly exceeded what would be expected if clay retention were only due to interstitial clay filling bed pore volume at the same concentration as the flow. Additionally, the aggradational phase showed substantially higher clay retention than the bypass phase in all runs. Bed-deposit samples from the variable-discharge run showed higher clay retention than the constant-discharge run with the same clay concentration.

DISCUSSION

The experiments run under constant, high-discharge conditions produced deposits similar to those typically considered diagnostic of variable flow conditions (e.g., clay drapes and flaser-like bedding). This suggests that the presence of clay drapes and lenses in channel deposits is an insufficient gauge of discharge intermittency or tidal influence in ancient rivers without other compelling evidence. Despite having a relatively low clay concentration, the variable-discharge experiment retained more clay than its constant-discharge counterpart. Clay drapes that formed in the variable-discharge run tended to be discontinuous because of erosion that occurred during re-activation of the bed as discharged increased. This suggest that the character of clay accumulations from truly intermittent flows might be differentiable from those generated in rivers with more constant discharge. However, results of these experiments suggest that the overall flux of fine-sediment through a system may be a dominant control on total fine-sediment retention in sandy riverbeds.

Clay in these experiments should have been transported as wash load and had limited interaction with the bed; however fine sediment was routinely deposited and preserved along with sandy bed material. These experiments were run in freshwater with kaolinite clay. Although such conditions are not strongly associated with flocculation, some clay aggregates were observed in each experiment and may have contributed to clay accumulation in the bed (Supplemental Videos). However, the majority of clay moving through the flume was suspended uniformly throughout the water column, so aggregates may not have been the primary source of clay extraction from the flow to the bed. Fine-sediment accumulations were most prevalent on the lee sides of individual bedforms downstream of the sediment wedge (e.g., Figure 2). This pattern contrasts with clay accumulation observed in some experiments where advective pumping and hyporheic exchange cause clay to be incorporated into the upstream side of dunes (e.g., Packman and MacKay, 2003), and suggests that the presence of the sediment wedge facilitated clay deposition in the experiments.

The sediment wedge may have initiated a flow-separation zone at its crest which might have promoted clay deposition in a recirculation zone immediately downstream of the wedge front. The prograding wedge also locally sequestered sand in the flume during the aggradational phase of the expeirment. The lower effective sand flux downstream of the wedge resulted in bedform-migration rates that were ~8 times slower during the aggradation phase (1.1-1.8 cm/s) than the bypass phase (8.6-12.0 cm/s). Although the concentration of clay supplied to the flow was constant throughout the runs, downstream of the wedge the concentration of clay relative to sand was much higher in the aggradational phase than the bypass phase. Enhanced fine-sediment deposition downstream of the sediment wedge is consistent with field data showing silt and clay accumulations downstream of bars in modern rivers and ancient deposits (Hajek et al., 2011; Lynds and Hajek, 2006).

The preservation of accumulated fine sediment (and bed material in general) was likely enhanced by an abrupt increase in local aggradation as the sediment wedge passed a given location in the flume. In field-scale systems bar progradation might rapidly bury slower-moving bedforms, thereby preserving them entirely. This contrasts the partial preservation of relatively fast-moving bedforms (i.e. the lowermost portion of some bedforms are preserved) due to stochastic variation in dune height (e.g., Paola and Borgman, 1991) or slow long-term aggradation (e.g., Leclair, 2002). Collectively, the results of our experiments suggest that, at field scales, morphodynamics of larger features like bars may play a significant role in controlling the deposition and preservation fine sediment and bed material in rivers.

These results have important implications for interpreting ancient fluvial deposits. First, the fraction of fine sediment preserved in ancient bed-material deposits may reflect the amount of fine sediment supplied to a watershed. This means that relative differences in the proportion of fine sediment within channel-bed sandstones may be useful for determining which ancient fluvial systems had particularly mud-prone sediment sources, especially when coupled with observations about the abundance, geometry, and preservation of reach-scale fine-sediment deposits like inter-bar mudstones and floodplain deposits (e.g., Lynds and Hajek, 2006). This information may be useful for testing hypotheses about relative cohesion among ancient systems and the relationship between clay supply and fluvial planform (e.g., van Dijk et al., 2013). Furthermore, constraining the fraction of fines present bed-material deposits will be helpful for more accurately predicting heterogeneity and compartmentalization in fluvial reservoirs. More work is needed to determine whether quantitative paleosediment-flux reconstructions could be achieved, but in the near term, these results indicate that the amount of silt and clay preserved in riverbed deposits may be sufficient for relative comparisons among ancient rivers and testing hypotheses about which systems had high vs. low clay and silt supplies.

CONCLUSIONS

Results of these experiments demonstrate that 1) low discharge is not a necessary condition for clay deposition in active river beds, 2) clay deposition increases with clay supply, and 3) clay retention in the bed is significantly higher during periods of bed aggradation than sediment bypass, particularly when aggradation is facilitated by bar migration. While variable discharge may enhance clay deposition for a given fine-sediment flux, our results show that significant fine-sediment accumulations in ancient channel deposits may primarily reflect supplied wash load rather than highly variable discharge, as is often interpreted. This indicates that interpreting high discharge variability, for example tidally influenced flows or seasonal stagnation, requires evidence beyond clay deposits. Our results suggest that the presence of migrating bar forms may facilitate clay deposition and preservation during high flow conditions. Measuring the concentration of clay in ancient river-bed deposits may provide an important avenue for reconstructing paleo-sediment supply, particularly the relative abundance of clays and silts transported by a system; this is a critical variable necessary for understanding past changes in source material or weathering rates and evaluating the how clay contributed to cohesion on ancient landscapes and on other planets.

APPENDIX

Supplemental data submitted.

ACKNOWLEDGMENTS

Support for this research was provided by the donors of the American Chemical Society Petroleum Research Fund, NSF Award #1455240, and student support from the Geological Society of America, American Association of Petroleum Geologists, and Penn State Geosciences to N.W. Without the incredible expertise and generosity of SAFL personnel, particularly Ben Erickson and Sara Mielke this work would not have been possible. We are grateful to E. Chamberlin and Macalester College students for helping run the experiments and thank C. Paola, R. Slingerland, T. Bralower, R. DiBiase, E. Greenberg, and S. Trampush for helpful discussions, and J. Pizzuto and M. Perillo for thoughtful and constructive reviews.

REFERENCES CITED

Baas, J. H., Best, J. L., and Peakall, J., 2011, Depositional processes, bedform development and hybrid bed formation in rapidly decelerated cohesive (mud-sand) sediment flows: Sedimentology, v. 58, p. 1953-1987.

Baas, J. H., Best, J. L., and Peakall, J., 2016, Predicting bedforms and primary current stratification in cohesive mixtures of mud and sand: Journal of the Geological Society of London, v. 173, p. 12-45.

Bhattacharya, A., 1997, On the origin of non-tidal flaser bedding in point bar deposits of the river Ajay, Bihar and West Bengal, NE India: Sedimentology, v. 44, p. 973-975.

Bierkens, M. F. P., and Weerts, H. J. T., 1994, Block hydraulic conductivity of cross-bedded fluvial sediments: Water Resources Research, v. 30, no. 10, p. 2665-2678.

Downs, P. W., Cui, Y., Wooster, J. K., Dusterhoff, S. R., and Booth, D. B., 2009, Managing reservoir sediment release in dam removal projects: An approach informed by physical and numerical modelling of non-cohesive sediment: International Journal of River Basin Management, v. 7, no. 4, p. 433-452.

Draut, A. E., and Ritchie, A. C., 2015, Sedimentology of new fluvial deposits on the Elwha River, Washington, USA, formed during large-scale dam removal: River Research and Applications, v. 31, p. 42-61.

Hajek, E. A., Lynds, R., and Huzurbazar, S., Comparing particle-size distributions in modern and ancient sand-bed rivers, *in* Proceedings AGU Fall Meeting, San Francisco, 2011, American Geophysical Union.

Hamm, N. T., Dade, W. B., and Renshaw, C. E., 2011, Fine particle deposition to porous beds: Water Resources Research, v. 47, no. 11, p. n/a-n/a.

Hampson, G. J., Royhan Gani, M., Sahoo, H., Rittersbacher, A., Irfan, N., Ranson, A., Jewell, T. O., Gani, N. D. S., Howell, J. A., Buckley, S. J., and Bracken, B., 2012, Controls on large-scale patterns of fluvial sandbody distribution in alluvial to coastal plain strata; Upper Cretaceous Blackhawk Formation, Wasatch Plateau, central Utah, USA: Sedimentology, v. 59, no. 7, p. 2226-2258.

Jackson, M. D., Yoshida, S., Muggeridge, A. H., and Johnson, H. D., 2005, Three-dimensional reservoir characterization and flow simulation of heterolithic tidal sandstones: AAPG Bulletin, v. 89, no. 4, p. 507-528.

Leclair, S., 2002, Preservation of cross-strata due to the migration of subaqueous dunes: an experimental investigation: Sedimentology, v. 49, p. 1157-1180.

Lynds, R., and Hajek, E., 2006, Conceptual model for predicting mudstone dimensions in sandy braided-river reservoirs: AAPG Bulletin, v. 90, no. 8, p. 1273-1288.

Martin, A. J., 2000, Flaser and wavy bedding in ephemeral streams: a modern and ancient example: Sedimentary Geology, v. 136, p. 1-5.

Matsubara, Y., Howard, A. D., Burr, D. M., Williams, R. M. E., Dietrich, W. E., and Moore, J. M., 2015, River meandering on Earth and Mars: A comparative study of Aeolis Dorsa meanders, Mars and possible terrestrial analogs of the Usuktuk River, AK, and the Quinn River, NV: Geomophology, v. 240, p. 102-120.

Packman, A. I., and Brooks, N. H., 2001, Hyporheic exchange of solutes and colloids with moving bed forms: Water Resources Research, v. 37, no. 10, p. 2591-2605.

Packman, A. I., and MacKay, J. S., 2003, Interplay of stream-subsurface exchange, clay particle deposition, and streambed evolution: Water Resources Research, v. 39, no. 4.

Paola, C., and Borgman, L. E., 1991, Reconstructing random topography from preserved stratification: Sedimentology, v. 38, no. 4, p. 553-565.

Plink-Bjorklund, P., 2015, Morphodynamics of rivers strongly affected by monsoon precipitation: Review of depositional style and forcing factors: Sedimentary Geology, v. 323, p. 110-147.

Steel, R. J., Plink-Bjorklund, P., and Aschoff, J., 2011, Tidal deposits of the Campanian Western Interior Seaway, Wyoming, Utah and Colorado, USA, *in* Davis, R. A. J., and Dalrymple, R. W., eds., Principles of Tidal Sedimentology: Netherlands, Springer, p. 437-471.

van Dijk, W. M., van de Lageweg, W. I., and Kleinhans, M. G., 2013, Formation of a cohesive floodplain in a dynamic experimental meandering river: Earth Surface Processes and Landforms, v. 38, no. 13, p. n/a-n/a.

Wilkerson, G. V., and Parker, G., 2011, Physical basis for quasi-universal relationships describing bankfull hydraulic geometry of sand-bed rivers: Journal of Hydraulic Engineering, v. 137, no. 7, p. 739-753.

Wooster, J. K., Dusterhoff, S. R., Cui, Y., Sklar, L. S., Dietrich, W. E., and Malko, M., 2008, Sediment supply and relative size distribution effects on fine sediment infiltration into immobile gravels: Water Resources Research, v. 44, no. 3, p. n/a-n/a.

FIGURE CAPTIONS

Figure 1. A) Diagram of experimental setup showing flume extent and the location of clay and sand delivery; water entered the flume on the left side and exited over the weir on the right side. Sand was supplied dry and clay was delivered from a mixing tank at different concentrations in each run at a rate of 1 l/s. Data reported here come from the active bed region. The measurement cart included sediment-sampling and ADV equipment (at 2.9 m) and videos and photographs were taken from through the sidewall of the flume at 3.25 m. B) Example of bed evolution in the Test Section of the flume during the Intermediate Concentration run (3x vertical exaggertation). Lines show bed topography every 30 minutes through the experiment (progressing from light green to dark green). Raw panel shows the full bed topography and the smoothed panel shows the same data averaged with a moving window of two average bedform lengths (50 cm). Arrows indicate the approximate position of the front of the sediment wedge at each time. All runs showed the same bed evolution; complete bed-evolution histories and experimental details are included in the supplemental material.

Figure 2. Example clay-deposit types found in experimental beds. Striped region defines the pre-run bed and the dashed line shows the transition from aggradation-phase deposits (below) to bypass-phase deposits (above). The high-concentration, constant-discharge run (A) had the largest visible clay deposits in the form of lenses and abundant continuous clay drapes. The

intermediate-concentration run (B) had smaller, less predominant clay lenses and continuous clay drapes. The low-concentration run (C) lacked clay lenses and had thin clay drapes. The variable-discharge run (D) showed more prominent clay drapes than its constant-discharge counterpart (C), but drapes were relatively discontinuous compared to those observed in other constant-discharge runs. All runs also contained intercalated, interstitial clay that was distributed throughout the bed.

Table. Summary of experimental bed deposit characteristics. Fine-sediment concentration is the concentration of clay in the flow during each run. Fine sediment deposits describe the dominant types of fine-sediment accumulations mapped in each experimental bed (Figure 2). Expected weight percent of fine sediment in the bed samples is the amount of interstitial clay expected in bed pore waters given the supplied concentration for each run. Aggradation and bypass fine sediment weight percent are the average of samples from each phase of each run. Full bed maps and sample data are included in the supplemental material, along with details of a constant-discharge control run that contained no supplied clay.

[1]GSA Data Repository item 201Xxxx, supplementary data including details of experimental conditions and analyses, is available online at www.geosociety.org/pubs/ft20XX.htm, or on request from editing@geosociety.org or Documents Secretary, GSA, P.O. Box 9140, Boulder, CO 80301, USA.

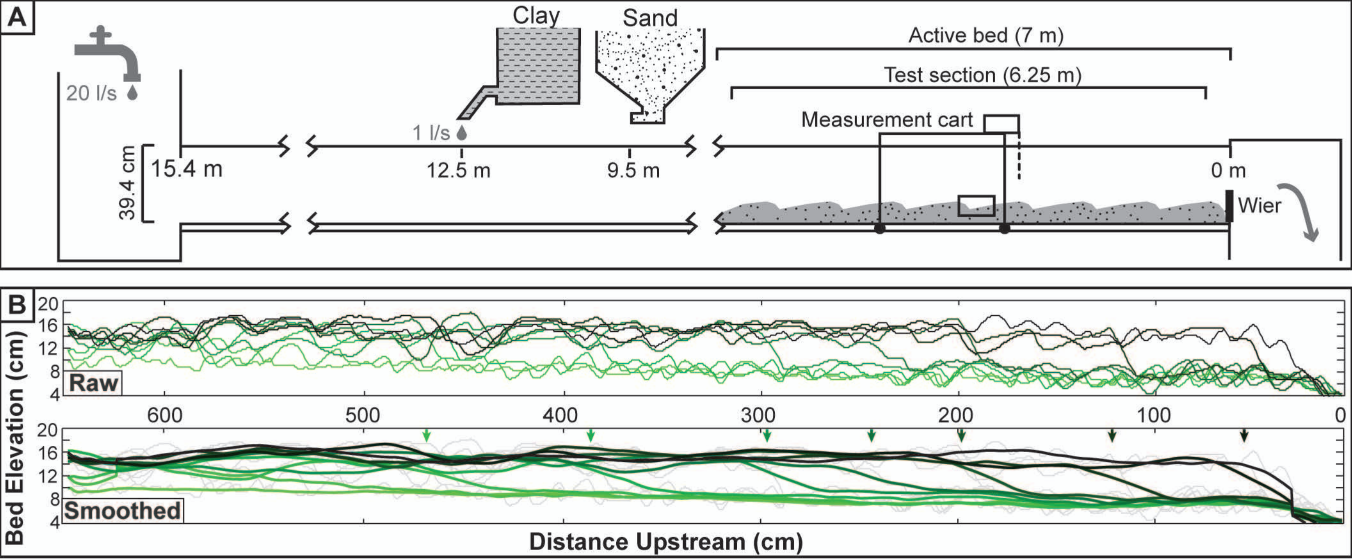
A
Clay
Sand
Active bed (7 m)
Test section (6.25 m)
20 l/s
1 l/s
Measurement cart
39.4 cm
15.4 m
12.5 m
9.5 m
0 m
Wier
B
Raw
Smoothed
Bed Elevation (cm)
Distance Upstream (cm)
20
16
12
8
4
600
500
400
300
200
100
0

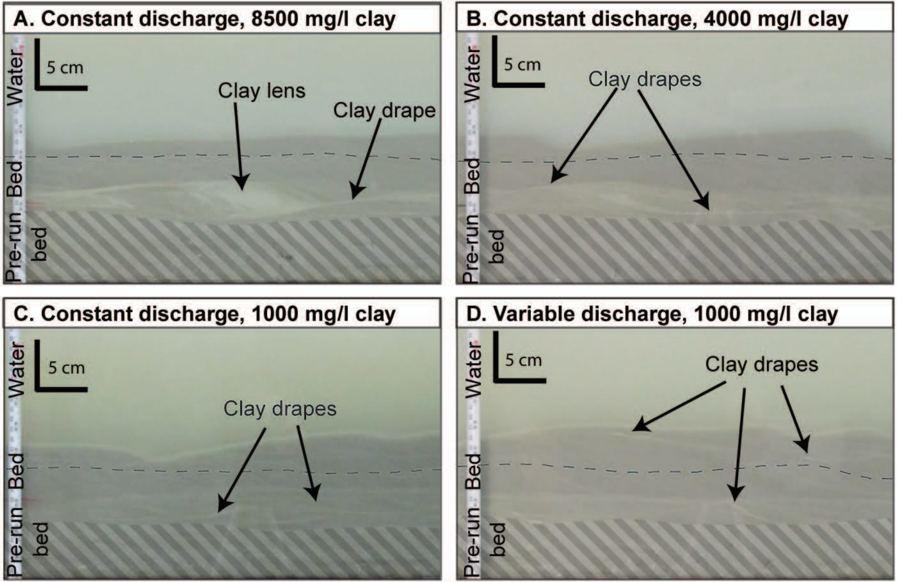
A. Constant discharge, 8500 mg/l clay
Water
5 cm
Clay lens
Clay drape
Bed
Pre-run bed
B. Constant discharge, 4000 mg/l clay
Water
5 cm
Clay drapes
Bed
Pre-run bed
C. Constant discharge, 1000 mg/l clay
Water
5 cm
Clay drapes
Bed
Pre-run bed
D. Variable discharge, 1000 mg/l clay
Water
5 cm
Clay drapes
Bed
Pre-run bed

	Fine-sediment concentration	Fine-sediment deposits	Fines in bed samples [wt%]		
			Expected	Aggradation	Bypass
Low concentration	1000 mg/l	Intercalated fines	0.02	0.06	0.05
Intermediate concentration	4000 mg/l	Drapes, intercalated fines	0.08	0.8	0.2
High concentration	8500 mg/l	Drapes, lenses, intercalated fines	0.17	2.2	0.4
Variable dishcharge	1000 mg/l	Disctoninuous drapes, intercalated fines	0.02	0.2	0.1

Data repository and supplemental information for Wysocki and Hajek: Is fine sediment in sandy riverbed deposits a proxy for paleo-sediment supply?

DESCRIPTION OF EXPERIMENTAL PROCEDURES:

Description of flume and sediment used in experiments

Experiments were conducted in the 24-in general purpose flume at the St. Anthony Falls Laboratory, University of Minnesota (http://www.safl.umn.edu/facilities/general-purpose-flumes-6-inch-20-inch-24-inch-flumes); see Figure 1 in the main manuscript. The flume is a feed style flume 15.42 meters long (50 ft) and 39.97 cm deep (15.5 in). Near the head box the flume is 61 cm and between 14.7 and 12.2 m, the flume narrowed from 61 cm to 30.5 cm. The flume was 30.5 cm-wide for from 12.2 m to the end (0 m) at the weir. The weir height for all runs was fixed at 16 cm. For each run, the initial sediment wedge extended from the outlet of the flume to 8 m and was graded to a slope of 0.004.

The sand feeder was positioned at 8.5 m and the sand feed rate was set at 15.0 g/s (a voltage of 356 on the auger box). This feed rate was verified before each run and prior to sand feed being turned off at the conclusion of each run. Based on water velocity and fall velocity of the median grain diameter sand (0.323 mm) the sand traveled 1.5-1.75 m before reaching the bed. The sand used in these experiments is AGSCO #40-#70 silica sand. This has a narrow distribution with D_{50}=0.323 mm, and a sorting coefficient of 1.2. A board was positioned below the feeder to disperse the sand supply, spreading it across the width of the flume.

Clay was delivered to the flume via two mixing tanks. First, clay was fully mixed and wetted in a mixing tank located on the floor above the flume. A clay slurry left this initial mixing tank and was delivered to a second 1 m^3 mixing tank positioned just above the flume at 12.5 m. In the second mixing tank, the clay slurry was diluted with city water supplied at a rate of 1 l/s and was mixed via propeller. The dilute clay mixture from the secondary mixing tank was then introduced to the flume at a rate of 1 l/s. Clay was added to the initial mixing tank in volumes that produced the desired final concentration, and the clay slurry was delivered to the secondary mixing tank at a rate to balance the 1 l/s discharge from the secondary mixing tank into the flume. The water level in the tank and sediment feed rate (especially when high) were variable and were monitored and adjusted frequently throughout the course of each run to maintain the appropriate clay concentration in the flume. The clay feed from the secondary take was run over a board to disperse the clay supply uniformly across the width of the flume; this also helped prevent the slurry from becoming a density flow. Clay used in this experiment was Cary Snobrite kaolin clay with a median grain diameter of 0.004 mm. There was no overlap between sand and clay grain size distributions.

The main water supply to the flume Mississippi River water sourced from the St Anthony Falls Lab main channel diversion.

Startup and shutdown procedures

Start-up checklist

- Set initial sediment wedge by scraping off all sediments from prior experiments and grading the slope at 0.004.
- Test sand and clay sediment feed rates.
- Wet sediment wedge for over an hour so that water fills all pore spaces. Using a very low discharge, slowly fill the flume to the level of the weir.
- Start camera.
- Increase the flow to the desired discharge. Lift up on hydraulic pump until plate is at correct location (marked).

- Start clay slurry feed.
    - Turn on hose and sediment feeder in secondary clay mixing tank.
- Turn on sand feed. This starts the official time.
- Note: Ideally clay and sand are turned on at the same time. This can be done with more than one person. The person downstairs turns the hose on, the person upstairs turns the clay feeder on then opens the ball valve. When the slurry enters the flume, the person downstairs turns on the sand feed.
- Check discharge by the water level going over the weir. Should be at 29 cm. if not, adjust discharge with hydraulic pump.

<u>Shut down procedures</u>

- Note time when sediment wedge reaches the weir and the entire bed is at bypass.
- Continue run for 15-30 minutes after this time and begin shut-down.
- Slightly decrease discharge so sand is no longer in suspended load regime.
- Turn off sand feed.
- Turn off clay feed.
    - Shut ball valve, turn off hose, turn off sediment feeder.
- Immediately turn off river water discharge.
- Open drain on the headbox so the flume slowly drains from both sides.
- When bed is drained (still water in the flume, just not above the bed surface) open drain on headbox fully to allow flume to fully drain.
- Turn fan on the bed. Fan is attached to the top of the flume with clips at 1.5 meters blowing upstream.
- Let bed dry over two nights.

<u>Procedures during run</u>

- Collect velocity measurements at 6/10 water depth for 5-10 minutes.
- Collect additional velocity profiles by measuring for one minute at increments of 2 cm water depth from the bed to the top of the flow. (This proved difficult with migrating bedforms.)
- Collect bed and water surface elevation measurements from measuring tape every 50 cm of the test section. Make water surface elevation measurements every 1 meter outside of the test section.
- Take photographs of the test section every 30 minutes (15 minutes after bed and water surface elevations).
    - These are taken 180 cm (~6 ft) away from the flume at points (for the left foot of the tripod) marked on a piece of tape on the floor.
- Suspended sediment samples
    - Samples are taken every 30 minutes by a rake of suspended sediment samplers (Photo), with active tubes spaced 5 cm apart.

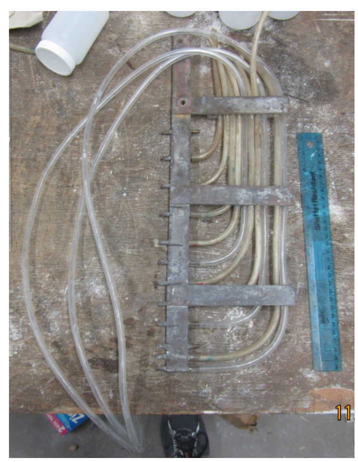

Photo: Suspended sediment sampler

    - Suspended sediment sample are collected at the 2 m position in the flume from 3 cm, 8 cm, and 13 cm above the bed.
    - Samples are taken by siphoning water through tubes and letting water enter 16 oz containers

    - Nearest dune location and dune height are noted
- Active bed material samples
    - Grab samples are taken every 30 minutes (with suspended sediment samples) taken with 8 oz containers.
    - Taken from top few centimeters of closest upstream dune to the 2 m position in the flume.
- Note the time when the prograding wedge reaches the weir and the entire bed is at bypass.
- Continue run for 15- 30 minutes.

Shutdown and startup procedures for variable flow run

- Follow shut-down procedures as normal with the exception of only turning down the clay feed before turning the river water off. Immediately after river water is turned off, shut down clayfeed and let the bed slowly drain naturally. Do not open the valve in the headbox.
- Allow clay to settle for prescribed time.
- To start flume, turn on clay feed to a very low discharge and slowly increase river water discharge (so as not to send a flood wave through the flume eroding the bed). When river discharge is up, turn on clay and sand feed as normal.

LINKS TO VIDEOS OF EACH EXPERIMENTAL RUN

High Concentration Run:
https://www.youtube.com/watch?v=94O93QsWivU
https://www.youtube.com/watch?v=_hLRHIdaPxI

Intermediate Concentration Run:
https://www.youtube.com/watch?v=wtui5OUFGvw
https://www.youtube.com/watch?v=nTdUC845o8Y

Low Concentration Run:
https://www.youtube.com/watch?v=-fE8_mEmQ0Q

Variable Discharge Run:
https://www.youtube.com/watch?v=N4nBBHzqulE
https://www.youtube.com/watch?v=XZfngqdCwZ8

EXPERIMENTAL CONDITIONS AND BED EVOLUTION:

Table DR1: Summary of experimental conditions and bed evolution for each run. Aggradation time is the total time the experiment experienced a net increase in average bed elevation in the test section (starting from the beginning of the experiment) and bypass time is the total time the experiment was run after the bed in the test section fully aggraded (i.e. no net increase in mean bed elevation).

	No Fines	Low Concentration	Intermediate Concentration	High Concentration	Variable Discharge
			EXPERIMENTAL CONDITIONS		
Water discharge (l/s)	21	21	21	21	Variable (see Table DR2)
Sand discharge (g/s)	15.0	15.0	15.0	15.0	15.0 (when water discharge > 0)
Clay concentration (mg/l)	0	1,000	4,000	8,500	1,000
Total run time (min)	303	272	277	253	262
Aggradation time (min)	239	239	262	236	247
Bypass time (min)	64	33	15	17	15
			BED EVOLUTION		
Bed aggradation rate (cm/min)	0.024	0.025	0.025	0.025	0.024
Total bed aggradation (cm)	6.1	6.1	6.8	6.4	6.6
Downstream wedge progradation rate (cm/s)	2.4	2.4	2.1	2.8	2.1
Mean bedform height (cm)	2.3	2.5	2.2	2.3	2.2
Bedform height standard deviation	1.5	1.4	1.4	1.2	1.2
Mean bedform migration rate (cm/s)					
Aggradational Phase	---	1.1	1.1	1.8	1.2
Bypass Phase	---	12.0	8.6	11.1	10.2

Table DR2: Run and stop (settling) times for the Variable Discharge run

	Part 1	Part 2	Part 3	Part 4	Part 5
Run time (min)	59	55	56	66	27
Settling time (min)	69	69	1010	179	End of run

Figure DR1: Bed aggradation throughout each run.
Bed elevation is the mean elevation of the bed (e.g., mapped profiles in Manuscript Figure 1 and Figure DR6). High = High Concentration Run, Int = Intermediate Concentration Run, Low = Low Concentration Run, Var = Variable Concentration Run, Nf = No Fines (control) Run.

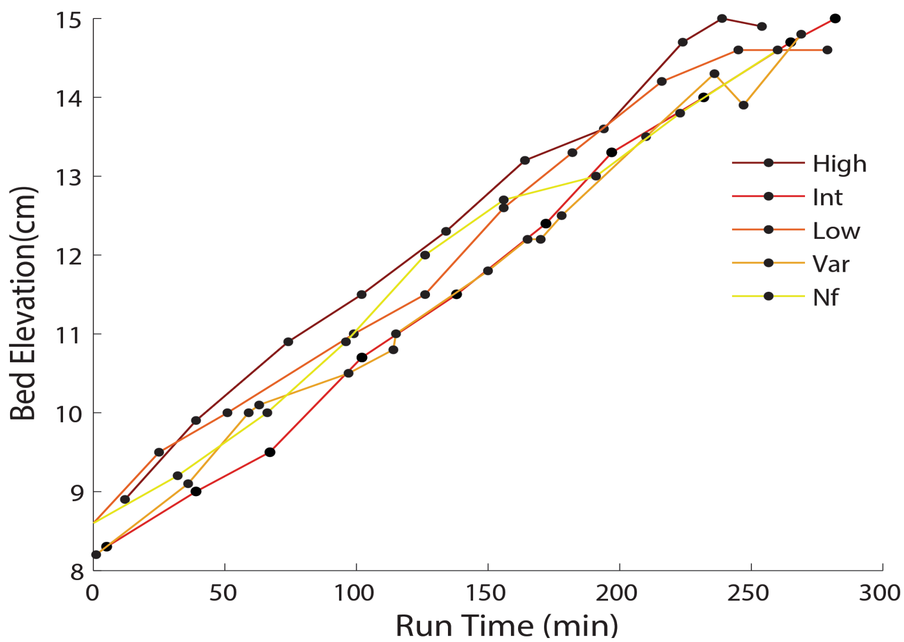

Figure DR2: Histogram of measured bedform heights for each run.
On bed-topography profiles mapped from photos every 30 mins throughout the experiment (Figure DR4), the height (elevation of crest minus elevation of trough) and length (distance between dune crests) of each bedform was measured. Number of bedforms measured for each experiment: No Fines (NF) = 188, Low Concentration (Low) = 202, Intermediate Concentration (Int) = 246, High Concentration (High) = 214, Variable flow (Var) = 420.

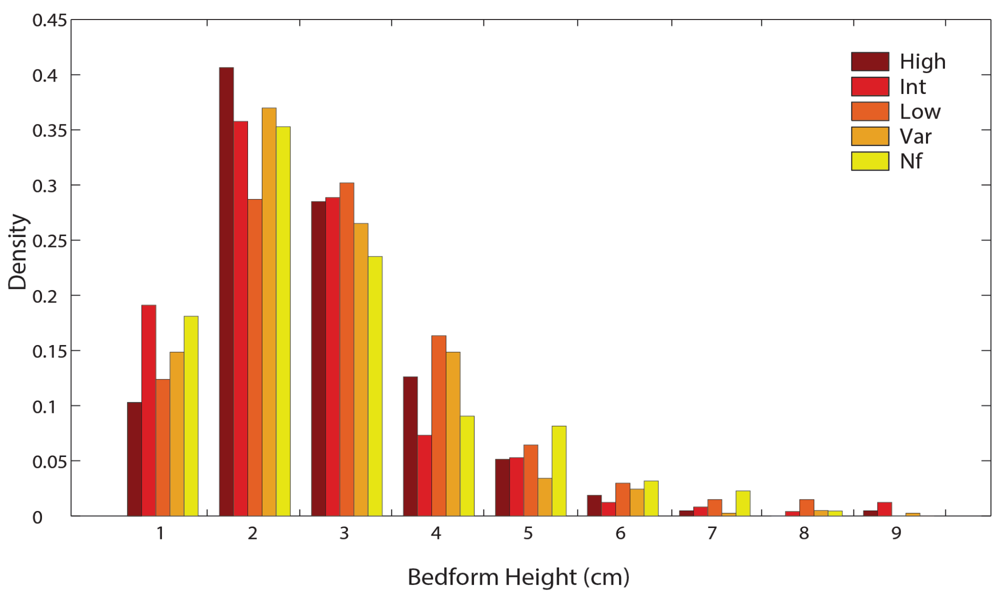

Experimental sediment-transport conditions

Figure DR3: Shield's diagram (after Wilkerson and Parker (2011)) showing experimental sediment-transport conditions.

Shields Stress (τ^*_{bf}) was calculated using Wilkerson and Parker's Equation 13:

$$\tau^*_{bf} = \frac{H_{bf}S}{RD_{50}}$$

where H_{bf} is the flow depth, S is the slope, R is the submerged specific gravity of sediment, and D_{50} is the median grain size.

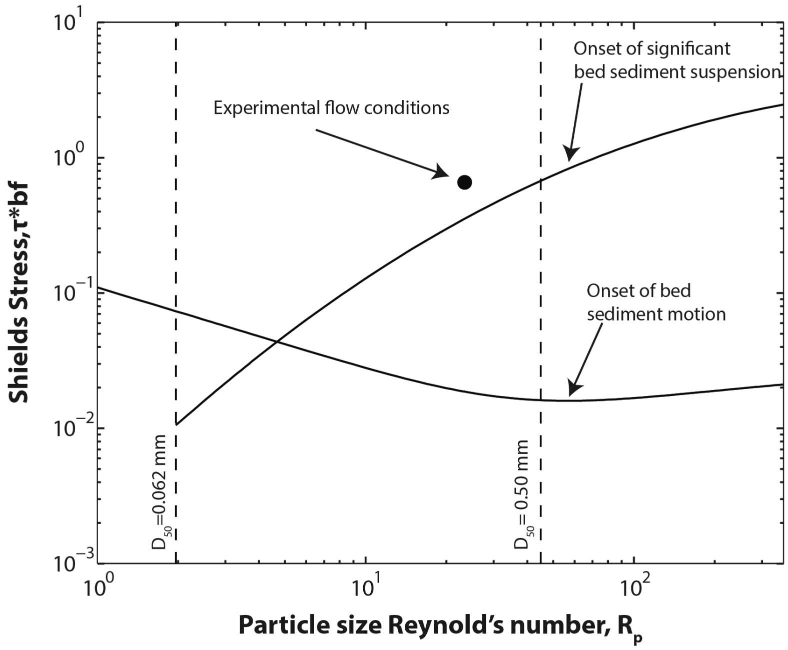

Fine sediment transport

Fine sediment supplied to the flume should have bypassed the entire flume as wash load. Given the slowest average water discharge in the suite of experiments (40 cm/s), and a settling velocity for clay in freshwater of 0.0002 cm/s (Sutherland et al., 2015), clay introduced at 12.5 m in the flume would have settled only 60 microns through the water column during its transport downstream in the experiments. Additionally, the concentration of clay in these experiments (0.5% by weight) was lower than the concentrations shown to induce significant changes in settling behavior of clay (either through flocculation or hindered settling, e.g., Sutherland et al., 2015) or the turbulence character of the flow (e.g., Baas et al., 2009).

Comparison with of experimental conditions with other flume experiments

Table DR3: Comparison of conditions in this study with other mixed sand-clay flume experiments.

Values for experiments in this study are averages of measurements taken throughout each run. Concentration (C) was imposed in each run. Flow depth (h) for each run is the average water-surface elevation minus the average bed elevation. Average flow velocity (U) was estimated by averaging ADV measurements throughout each run. Slope is the average of measured water-slopes during each run. Froude (Fr) and Reynolds (Re) numbers are estimated using flow depth and velocity and standard values for water density and viscosity. Baas et al. experiments include those that match the experimental conditions of this study most closely. Baas et al. classify the flow structure of their runs using detailed Ultrasonic Doppler velocimetry profiling (listed in Notes column). All data were reported in their 2009 and 2011 papers; slope value for the 2011 run is a bed slope. For Packman and MacKay experiments, slope is reported as "energy grade line"; Fr and Re were not reported in their paper, so we estimated values for each run (italics).

	Run	**C (mg/l)**	**h (cm)**	**U (cm/s)**	**Slope**	**Fr**	**Re**	**Notes**
Wysocki & Hajek (this study)	No Fines (control)	0	17.5	45	0.0018	0.34	78750	Variable Flow Run values are for high flow conditions
	Low Conc.	1000	16.6	50	0.0019	0.39	83000	
	Intermed. Conc.	4000	15.1	40	0.0016	0.33	60400	
	High Conc.	8500	14.9	60	0.0019	0.50	89400	
	Variable Flow	1000	16.2	46	0.0020	0.37	74520	
Baas et al. (2011)	1	5200	15.1	46.5	0.00138	0.38	69939	Turbulent Flow
Baas et al. (2009)	3-1	500	14.5	43.9	0.00018	0.37	63599	Turbulent Flow
	3-2	4000	15.7	42.6	0.00029	0.34	65256	Turbulent Flow
	3-3	9600	15.5	41.4	0.00029	0.34	63473	Turbulence-Enhanced Transitional Flow
	4-2	4000	15.4	55.9	0.00029	0.44	86023	Turbulent Flow
	4-3	9800	15.1	55.7	0.00029	0.43	83182	Turbulent Flow
	5-2	4200	15.0	70.4	0.00029	0.58	105467	Turbulent Flow
Packman and MacKay (2003)	1	230, 460, 230	8.7	23.3	0.064	*0.25*	*20271*	Pulsed injections of clay
	2	280, 230, 220	11.8	23.7	0.044	*0.22*	*27966*	Pulsed injections of clay
	3	810	8.6	23.6	0.064	*0.26*	*20296*	Pulsed injection of clay

Figure DR4: Comparison of flow conditions in experiments from this study to the phase diagram presented in Baas et al. (2009).

Approximate range of experiments in this study shown in the gray box. Note that their diagram is for flow depths from 0.13-0.16 m, and that some of our experiments are slightly above those depths. Baas et al. Figure 17.

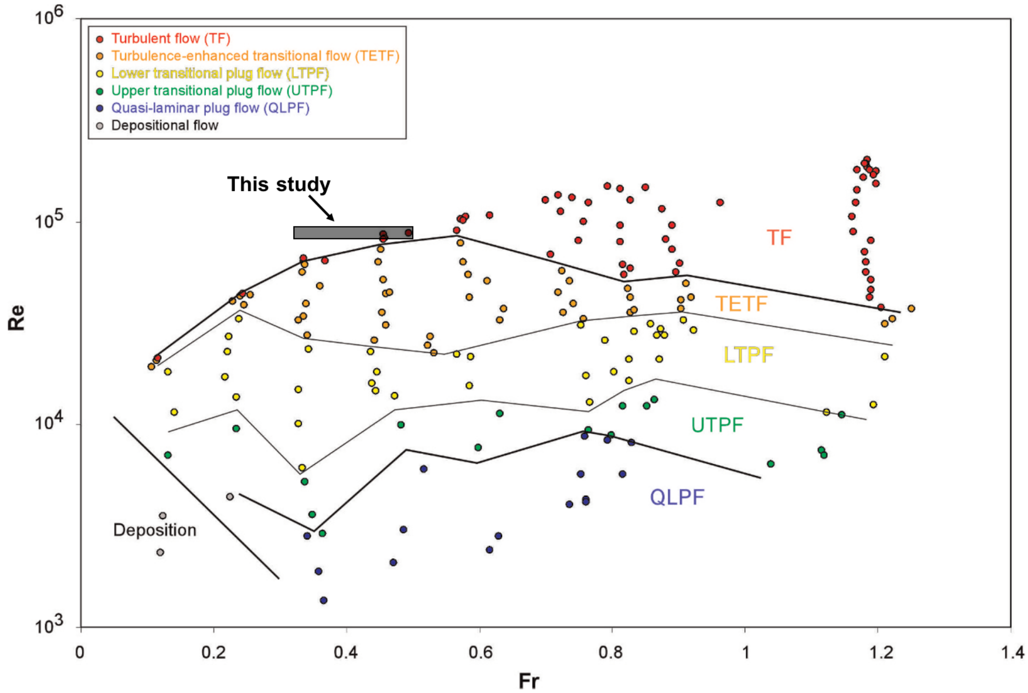

Figure DR5: Comparison of experiments in this study to the clay flow phase diagram of Baas et al. (2009).

Approximate range of experiments in this study is shown in the orange box. U is the depth-averaged flow velocity and C is the depth-average volume concentration of clay. Baas et al. Fig 15A.

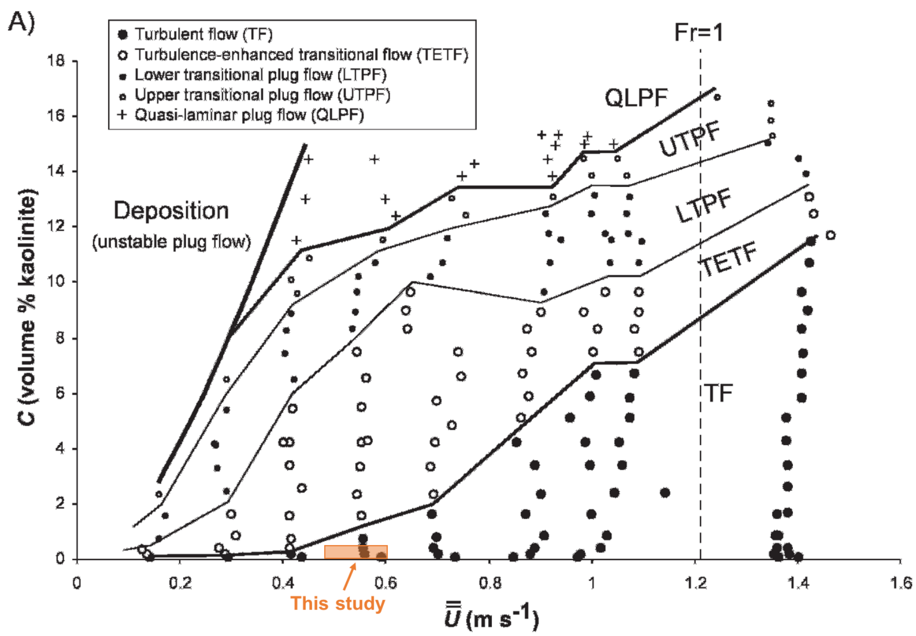

Figure DR6: Topographic profiles through time of each experiment.
The top figure in each set is the measured values and the bottom figure is smoothed profiles, which is accomplished with a moving window two average dune lengths (50cm); colors show profiles every 30 minutes (light to dark, as in Manuscript Figure 1). Vertical exaggeration is 3x.

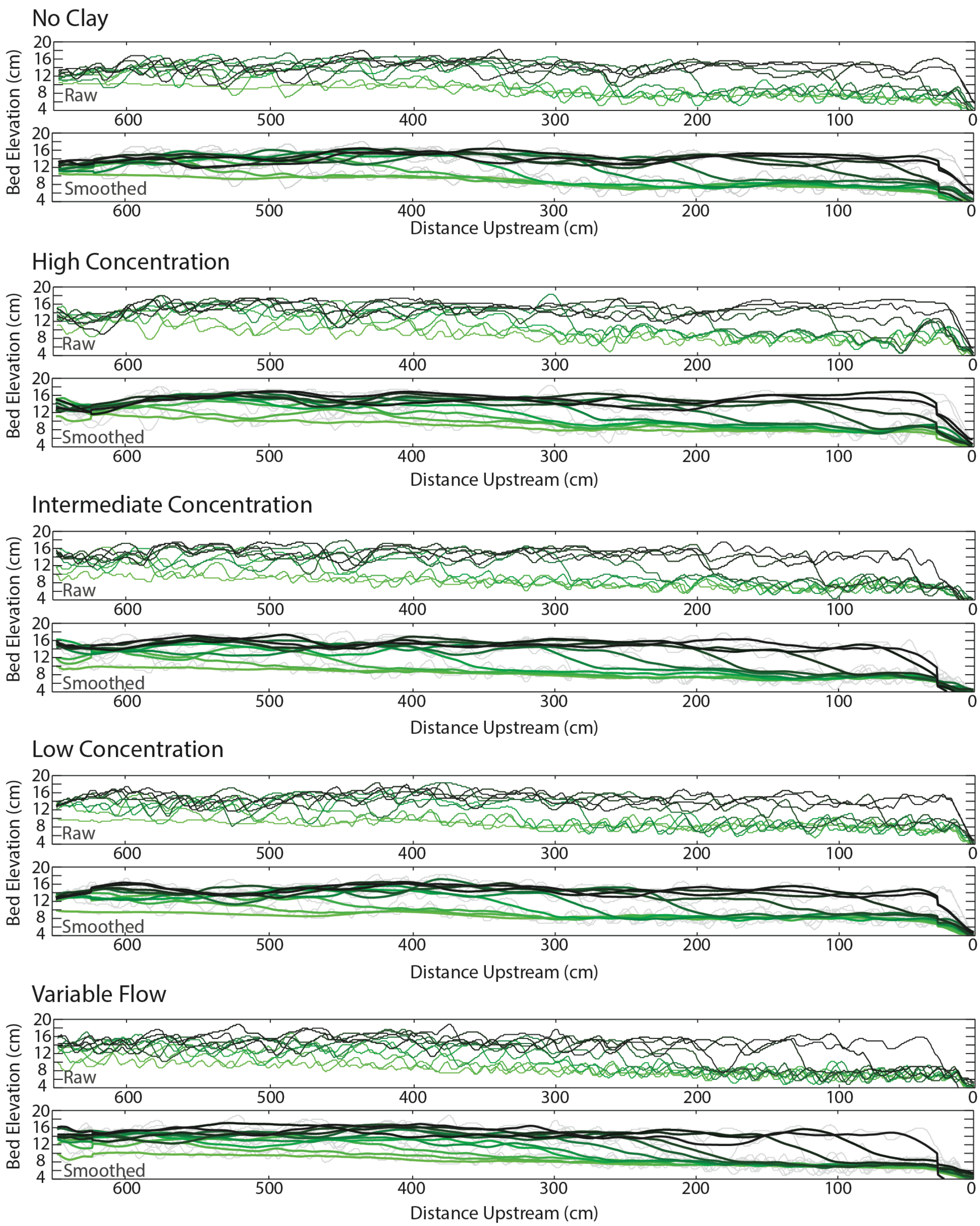

Figure DR7: Turbulence intensity calculated from ADV data from each run.
There is no evidence of damping of turbulence at high clay concentration.

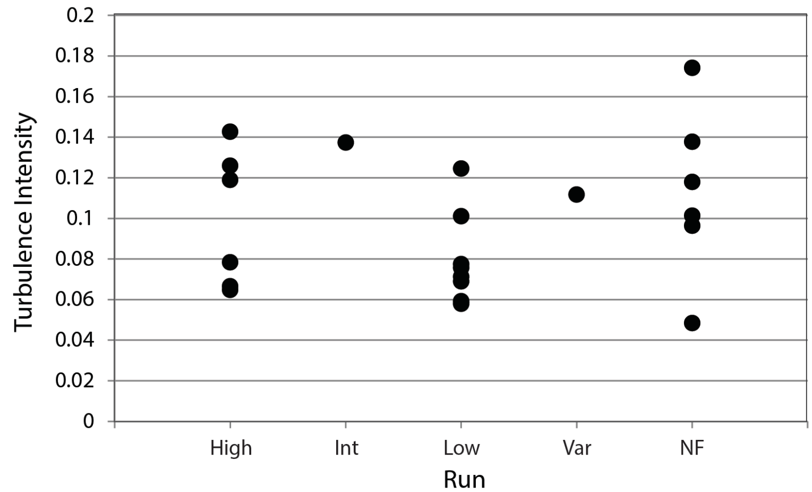

WinADV was used to process ADV data. Data were filtered using the automatic despiking program and used to calculate Turbulence Intensity (TI):
Turbulence intensity (TI)

$$TI = \frac{u'}{U} = \frac{\sqrt{\frac{1}{3}\left(u_x'^2 + u_y'^2 + u_z'^2\right)}}{\sqrt{U_x^2 + U_y^2 + U_z^2}}$$

where u' is the root mean square of the turbulent velocity fluctuations and U is the mean velocity.

Figure DR8: Suspended sediment concentration profiles.
Experiments show a generally well-mixed clay concentration throughout the water column. Clay concentration varies during a run, but there was no overlap in clay concentration between runs.

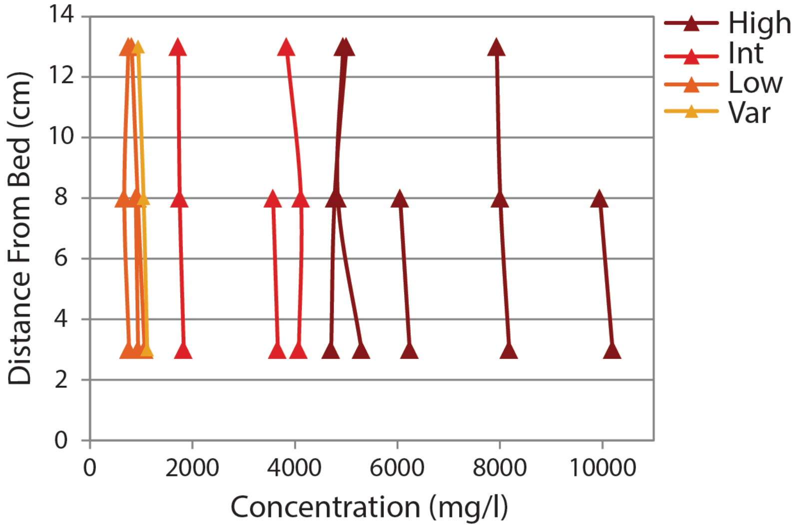

Figure DR9: Example images of clay aggregates in experimental runs.
Kaolinite flocs (white dots) in both the low-concentration run (A) and in the high-concentration run (B). Along the flume wall, in videos, there was evidence of flocculation in all runs, with more in the high-concentration experiment. However, clay flocculation was not did not occur at a level that changed the overall concentration of clay recorded in each experiment (Figure DR8), so it was not the dominant mode of clay transport in any of the runs. This is consistent with flocculation conditions documented in other experiments, where the conditions in this study (freshwater with clay concentrations <0.5 wt %) are below reported thresholds for significant flocculation (e.g., > 3.0 wt % in fresh water in Sutherland et al. (2015))

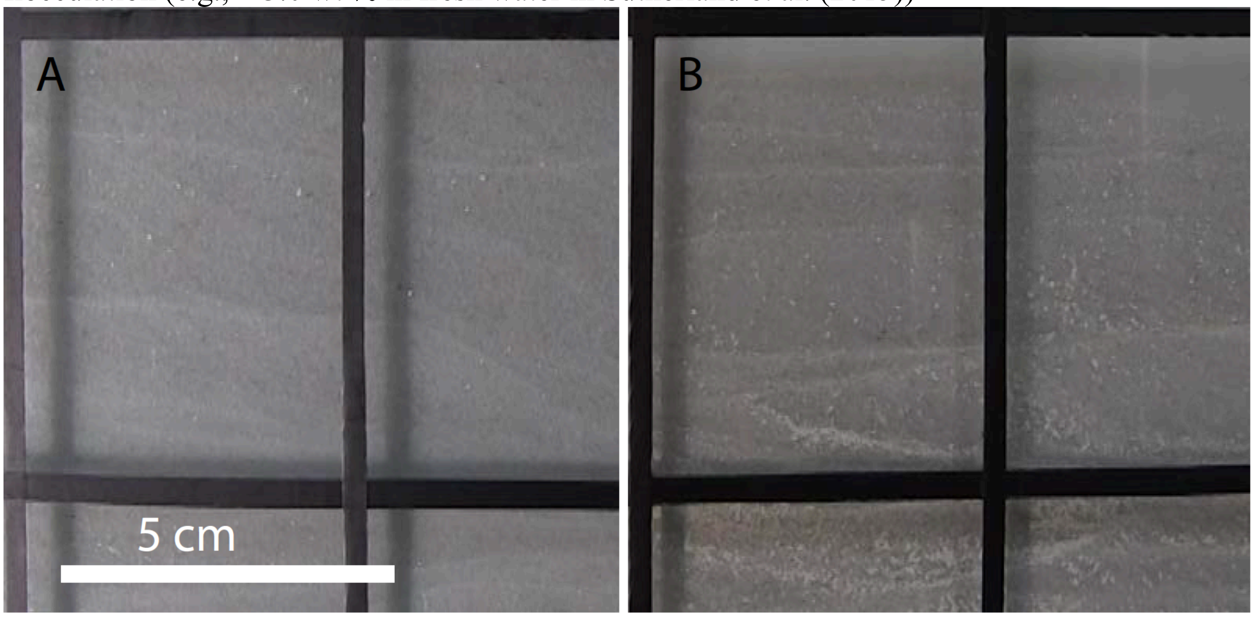

DEPOSIT CHARACTERISTICS AND CLAY ACCUMULATIONS:

Table DR4: Experimental deposit characteristics and clay-mapping results.

Run description	**No Fines**	**Low Concentration**	**Intermediate Concentration**	**High Concentration**	**Variable Discharge**
			GENERAL DEPOSIT CHARACTERISTICS		
Aggradation phase deposit thickness (cm)	4.3	4.2	4.6	5.1	5.0
Bypass phase deposit thickness (cm)	3.0	2.6	3.5	3.0	3.2
Total deposit cross-sectional area (cm^2)	4313	4533	4627	4737	5230
Aggradation phase deposit cross-sectional area (cm^2)	2549	2554	2596	3022	3250
Bypass phase deposit cross-sectional area (cm^2)	1765	1976	2032	1664	2010
Fraction of total deposit formed during aggradational phase	0.59	0.56	0.56	0.64	0.62
			CLAY ACCUMULATIONS		
Types of clay accumulations	None	None (small drapes near weir downstream of test section)	Continuous clay drapes, abundant intercalated clay	Continuous clay drapes, clay-rich lenses, abundant intercalated clay	Discontinuous clay drapes
Percent of total run deposit					
Intercalated clay	N/A	0	34	40	0
Drapes	N/A	0.1	8	12	1
Clay rich lenses	N/A	0	0	6	0
Percent of aggradation phase deposit					
Intercalated clay (%)	N/A	0	61	62	0
Drapes (%)	N/A	0.1	14	19	1
Clay rich lenses (%)	N/A	0	0	10	0

BED DEPOSIT SAMPLING

After each experiment, the bed was slowly drained and allowed to dry for two days prior to excavation. At this point the bed was dry enough to excavate without significantly collapsing. Bed-deposit samples and photographs were taken from the middle of the flume at various locations at different depths (Table 3) in order to capture samples deposited during both bypass and aggradation phases. These samples were taken with a 7cm x 7cm excavator tool, which allowed for bulk sediment samples. Bed-deposit samples were then wet-sieved to determine the fraction of clay.

Table DR5: Bed-deposit sample locations and weight percent of clay in the sample. Depositional phase and type of clay accumulations captured by each sample are noted. Qualitative sample descriptions describe the nature sample after being oven dried. Sands in some samples were clumped together and had to be manually disaggregated after sampling, indicating abundant clay. The NF run was a control experiment conducted with no clay discharge. Clay-sized material detected in that run came from the water (supplied from the Mississippi River via the St. Anthony Falls Lab main-channel diversion) or residuum within the sand supply.

Sample number	Run	Location (m)	Depth (cm)	Total weight (g)	Clay weight (g)	Clay %	Phase and clay types captured	Qualitative sample description
NF-1	NF	2.00	12.5-15.5	536.56	0.06	0.011	bypass	loose sand
NF-2	NF	2.00	9.5-12.5	523.92	0.08	0.015	aggradation	loose sand
NF-3	NF	5.00	12.0-15.0	491.25	0.07	0.014	bypass	loose sand
H-1	High	2.80	11.5-14.5	748.70	5.22	0.697	bypass	sticky/clumpy
H-2	High	2.80	8.5-11.5	825.56	16.87	2.044	aggradation. Clay drapes	hard
H-3	High	5.60	11.5-14.5	692.41	2.22	0.321	bypass	sticky/clumpy
H-4	High	5.60	8.5-11.5	778.64	2.46	0.316	bypass	sticky/clumpy
H-5	High	1.70	7.0-10.0	787.79	33.37	4.236	aggradation. Part of clay rich lens	hard
I-1	Int	3.35	11.5-14.5	716.00	1.50	0.210	bypass	loose with clumps
I-2	Int	3.35	8.0-11.0	833.63	3.47	0.416	split	sticky/clumpy
I-3	Int	2.35	11.0-14.0	783.41	2.25	0.288	bypass	loose with clumps
I-4	Int	2.35	7.0-10.0	859.58	15.58	1.813	aggradation. Clay drapes	hard
I-5	Int	4.60	12.5-15.5	700.41	1.46	0.209	bypass	loose with clumps
I-6	Int	4.60	8.5-11.5	901.94	1.97	0.218	split	loose with clumps
L-1	Low	1.80	11.0-14.0	746.79	0.35	0.047	bypass	loose sand
L-2	Low	1.80	7.5-10.5	799.44	0.51	0.064	aggradation	loose sand
L-3	Low	4.10	11.0-14.0	824.75	0.38	0.046	bypass	loose sand
L-4	Low	5.50	11.0-14.0	419.72	0.23	0.055	split (mostly bypass)	loose sand
V-1	Var	3.70	11.5-14.5	717.34	0.43	0.060	bypass	loose sand
V-2	Var	3.70	8.0-11.0	871.74	2.00	0.229	aggradation. Part of clay drape	loose sand with clumps
V-3	Var	5.25	11.5-14.5	778.63	0.51	0.065	bypass	loose sand
V-4	Var	5.25	8.5-11.5	791.50	0.74	0.093	aggradation	loose sand
V-5	Var	2.00	7.5-10.5	896.84	1.74	0.380	aggradation. Part of clay drape	loose sand with clumps

Bed Deposit Mapping Description and Images

Clay accumulations and bed areas are mapped on the vertically exaggerated images. Overlain topographic profiles and bed elevation points taken during the run helped determine which sediment was deposited during the bypass vs. aggradation phase. Clay accumulations were mapped on photographs of the bed. Clay accumulations appear whiter than the background sand, which is a tan color. Lighter colored sand indicates a higher abundance of intercalated clay (verified with weight percents of individual samples from these regions). Long and thin accumulations of clay were mapped as drapes and larger, thicker deposits were mapped as clay lenses. Bed areas of each type of clay accumulation were quantified using image analysis tools in Matlab.

Figure DR10: Photographs and mapped clay accumulations of each run as seen through the glass wall of the flume.

(Next pages) Vertical exaggeration is 3x. The y-axis is depth in centimeters. Hatched area is pre-run sediment. White areas are obstructed views of the bed. Sample locations are noted by black boxes. Each experiment (A-D) includes the following: i) composite photograph of test section through glass panel, ii) map of clay accumulations preserved in the bed (black) and definition of aggradational phase area (dark gray) and bypass phase area (light gray), and iii) map of different types of clay accumulations observable in the bed including, intercalated clay (dark gray), clay drapes (black), and clay rich lenses (red).

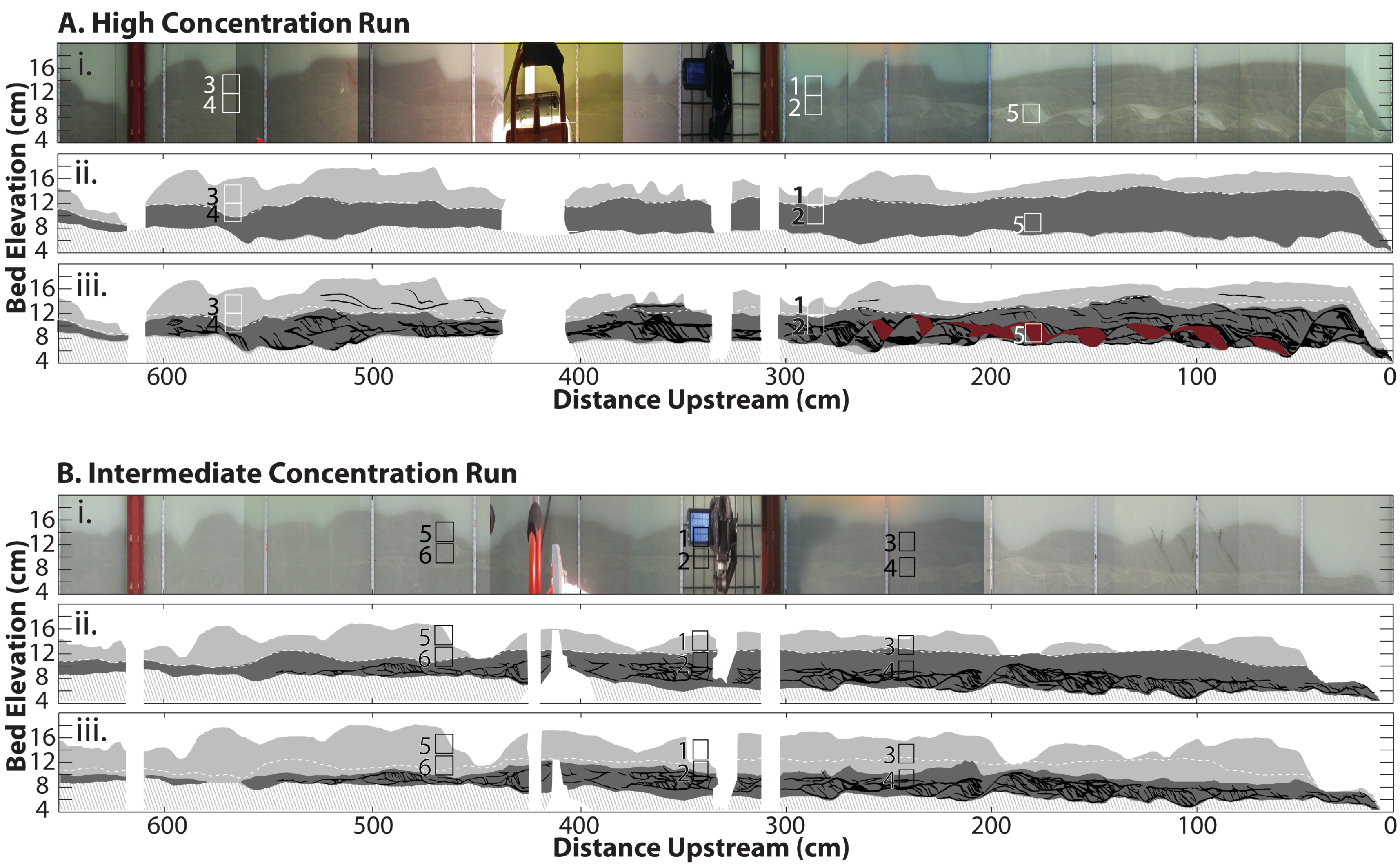
A. High Concentration Run
i.
ii.
iii.
Bed Elevation (cm)
Distance Upstream (cm)
B. Intermediate Concentration Run
i.
ii.
iii.
Bed Elevation (cm)
Distance Upstream (cm)

C. Low Concentration Run

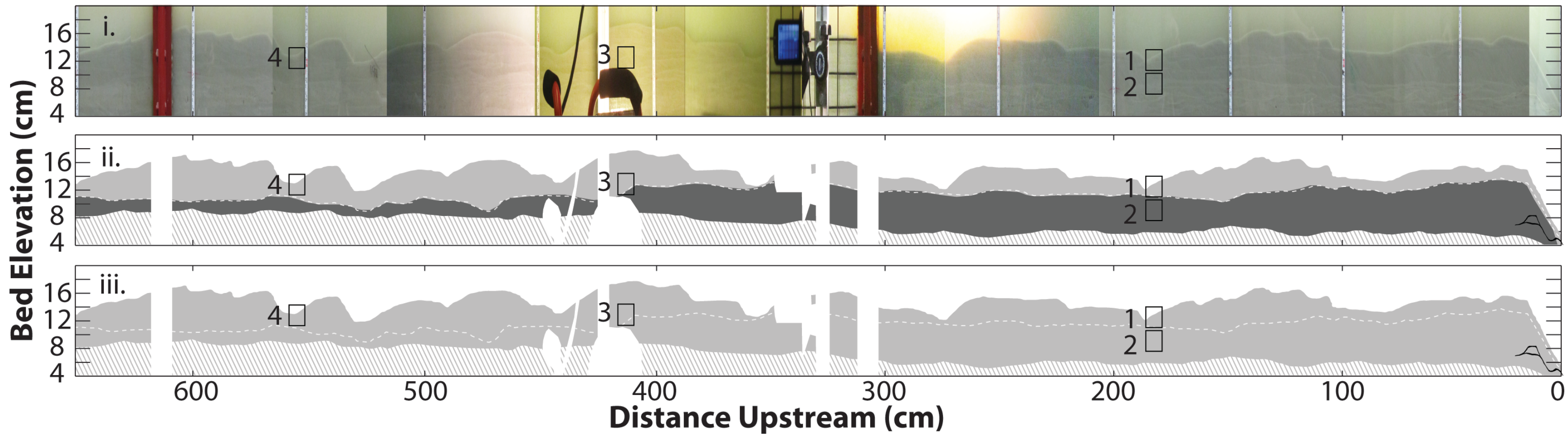

D. Variable Discharge Run

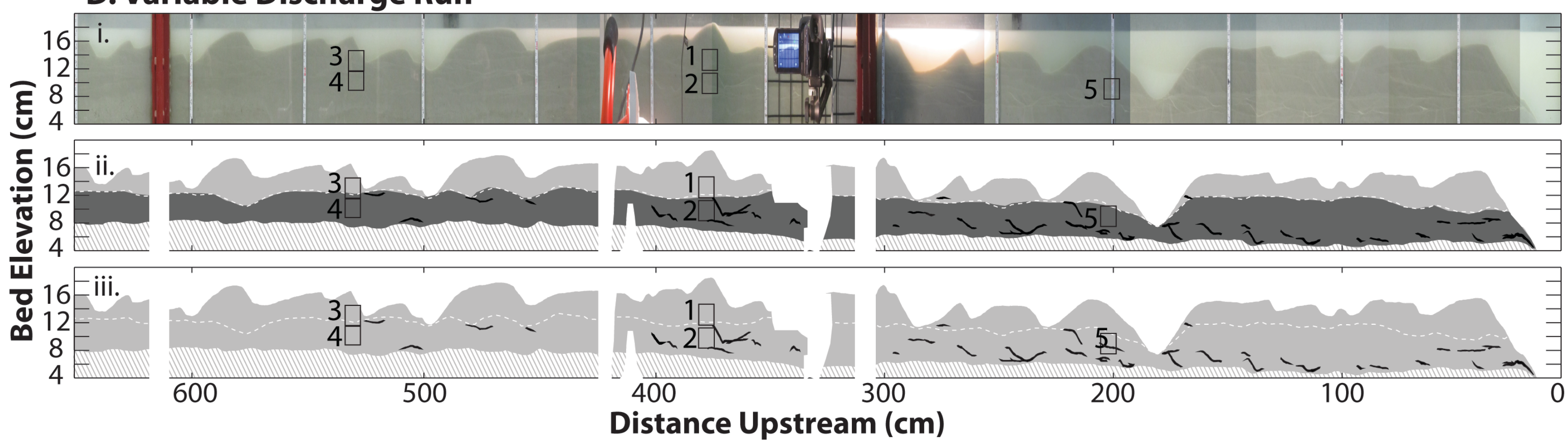

REFERENCES

Baas, J. H., Best, J. L., and Peakall, J., 2011, Depositional processes, bedform development and hybrid bed formation in rapidly decelerated cohesive (mud-sand) sediment flows: Sedimentology, v. 58, p. 1953-1987.

Baas, J. H., Best, J. L., Peakall, J., and Wang, M., 2009, A phase diagram for turbulent, transitional, and laminar clay suspension flows: Journal of Sedimentary Research, v. 79, p. 162-183.

Packman, A. I., and MacKay, J. S., 2003, Interplay of stream-subsurface exchange, clay particle deposition, and streambed evolution: Water Resources Research, v. 39, no. 4.

Sutherland, B. R., Barrett, K. J., and Gingras, M. K., 2015, Clay settling in fresh and salt water: Environmental Fluid Mechanics, v. 15, no. 1, p. 147-160.

Wilkerson, G. V., and Parker, G., 2011, Physical basis for quasi-universal relationships describing bankfull hydraulic geometry of sand-bed rivers: Journal of Hydraulic Engineering, v. 137, no. 7, p. 739-753.